Abnormal mineralization of the Ts65Dn Down syndrome mouse appendicular skeleton begins during embryonic development in a *Dyrk1a*-independent manner

Joshua D. Blazek[1], Ahmed M. Malik[1], Maeve Tischbein[2], Maria L. Arbones[3], Clara S. Moore[2] and Randall J. Roper[1,4]

[1] Department of Biology, Indiana University-Purdue University Indianapolis and Indiana University Center for Regenerative Biology and Medicine, 723 W. Michigan Street, SL306, Indianapolis, IN 46202, USA

[2] Department of Biology, Franklin and Marshall College, PO Box 3003, Lancaster, PA 17604, USA

[3] Department of Developmental Biology, Institut de Biologia Molecular de Barcelona IBMB-CSIC, and Centro de Investigación Biomédica en Red de Enfermedades Raras (CIBERER), Barcelona 08028, Spain

[4] Corresponding Author

Randall J. Roper, Ph.D.
Department of Biology
Indiana University-Purdue University Indianapolis
723 W. Michigan Street
SL 306
Indianapolis, IN 46202

Phone: (317) 274-8131
Fax: (317) 274-2846
rjroper@iupui.edu

Grant information: This work was supported by an Honors Program Research Fellowship (AM and RJR), an NSF GK-12 fellowship NSF-DGE 0742475 (JDB), the William and Lucille Hackman Scholars Program (MT and CSM), the Benedict Miller Foundation (CSM), the Franklin and Marshall Leser Fund (MT), and the Jerome Lejeune Foundation (RJR).

Abstract

The relationship between gene dosage imbalance and phenotypes associated with Trisomy 21, including the etiology of abnormal bone phenotypes linked to Down syndrome (DS), is not well understood. The Ts65Dn mouse model for DS exhibits appendicular skeletal defects during adolescence and adulthood but the developmental and genetic origin of these phenotypes remains unclear. It is hypothesized that the postnatal Ts65Dn skeletal phenotype originates during embryonic development and results from an increased *Dyrk1a* gene copy number, a gene hypothesized to play a critical role in many DS phenotypes. Ts65Dn embryos exhibit a lower percent bone volume in the E17.5 femur when compared to euploid embryos. Concomitant with gene copy number, qPCR analysis revealed a ~1.5 fold increase in *Dyrk1a* transcript levels in the Ts65Dn E17.5 embryonic femur as compared to euploid. Returning *Dyrk1a* copy number to euploid levels in Ts65Dn, *Dyrk1a*$^{+/-}$ embryos did not correct the trisomic skeletal phenotype but did return *Dyrk1a* gene transcript levels to normal. The size and protein expression patterns of the cartilage template during embryonic bone development appear to be unaffected at E14.5 and E17.5 in trisomic embryos. Taken together, these data suggest that the dosage imbalance of genes other than *Dyrk1a* are involved in the development of the prenatal bone phenotype in Ts65Dn embryos.

Running title: Origin of the Ts65Dn bone phenotype

Key words: Down syndrome, bone development, trisomy, dosage compensation, *Dyrk1a*

1. Introduction

Down syndrome (DS) or Trisomy 21 (Ts21) results from the presence of an extra copy of human chromosome 21 (Hsa21) and occurs in approximately 1/700 live births (Parker et al., 2010). The dosage imbalance of genes on Hsa21 leads to subsets of over 80 phenotypes that are clinically associated with DS and vary in severity and penetrance on an individual basis (Deutsch et al., 2005; Epstein, 2001). Individuals with DS exhibit alterations in the development and maintenance of their appendicular skeletons both pre- and postnatally (de Moraes et al., 2008; Keeling et al., 1997). Ultrasound measurements of the long bones during the second trimester where fetuses with DS exhibit shortened humerus and femur lengths suggest changes in prenatal DS bone development (Gray et al., 2009; Longo et al., 2004; Weisz et al., 2008). Postnatally, individuals with DS exhibit severe reductions in stature resulting from alterations in the normal cycle of skeletal growth during adolescent development (de Moraes et al., 2008). Furthermore, the mineral properties of bone are altered in individuals with DS. Individuals with DS exhibit a reduction in areal bone mineral density (BMD) in the spine, hip, and total body (Guijarro et al., 2008), as well as decreased strength in the femoral neck (Baptista et al., 2005). These deficiencies in bone mineral density are likely responsible for the increased risk of osteoporosis in both male and female individuals with DS (Center et al., 1998; Schrager, 2004; van Allen et al., 1999). Despite a gross structural understanding of the appendicular skeletal phenotypes, little is known about the origin and consequences of altered bone development in individuals with DS.

The Ts(17^{16})65Dn (Ts65Dn) mouse model is the most widely used model in the study of DS. Ts65Dn mice contain segmental trisomy for mouse chromosome 16 (Mmu16) resulting in three copies of approximately half of the gene orthologs triplicated in Ts21 (Davisson et al., 1993; Sturgeon and Gardiner, 2011). Ts65Dn mice exhibit several phenotypes similar to those observed in humans with DS including cognitive impairment, craniofacial and skeletal abnormalities, and cardiac anomalies (Blazek et al., 2011; Moore, 2006; Reeves et al., 1995; Richtsmeier et al., 2000) and have been instrumental in understanding the developmental origin of DS phenotypes. Ts65Dn embryos exhibit attenuated growth at E9.5 and E13.5, as measured by volume, crown-rump length and area, and this deficit continues through adolescence, as trisomic mice are significantly smaller by mass when compared to euploid littermates at postnatal day 0 (P0) and P6 (Blazek, 2010; Roper et al., 2006). Ts65Dn mice exhibit a reduction

in cell number and volume in the mandibular precursor at E9.5 and E13.5, deficits hypothesized to contribute the reduced mandible phenotype observed postnatally (Billingsley et al., 2013; Roper et al., 2009).

Previously, we identified an abnormal appendicular skeletal phenotype in 6 and 16 week old Ts65Dn mice. Ts65Dn mice exhibited reduced BMD, altered trabecular microarchitecture, and decreased mineralization compared to euploid mice, suggesting that trisomy significantly alters the normal development and maintenance of the appendicular skeleton (Blazek et al., 2011). Additional work on the Ts65Dn appendicular skeletal phenotype corroborated our findings and identified deficiencies in osteoclast and osteoblast number likely contributing to the weakened bone phenotype observed in Ts65Dn mice (Fowler et al., 2012). We observed that alterations in bone mineral density and trabecular microarchitecture were more severe at 6 weeks than 16 weeks of age in Ts65Dn mice and this suggested that alterations in bone growth would be detectable during early postnatal development and may originate embryonically. The development of the appendicular skeleton occurs via endochondral ossification where a cartilage template is formed and later replaced by mineralized bone during development. After the initial establishment and growth period, a coordinated process involving bone resorption and bone formation, known as remodeling, occurs continuously throughout life to maintain homeostasis in the appendicular skeleton. Based on the prenatal origins of many abnormalities associated with DS (Moore and Roper, 2007) and the differences observed in the bone phenotypes between 6 and 16 weeks of age, we hypothesized that the Ts65Dn appendicular skeletal phenotype originates during embryonic development.

In addition to the lack of knowledge regarding the origin of the Ts65Dn bone phenotype, the gene-phenotype relationships leading to skeletal deficits in DS are equally uncharacterized. It has been hypothesized that dual specificity tyrosine threonine kinase 1a (*DYRK1A),* found in three copies in humans with DS and Ts65Dn mice, contributes to several DS phenotypes, including skeletal abnormalities, via its interaction with the trisomic gene product of regulator of calcineurin 1 (*RCAN1*) and the Nuclear factor of activated T-cells (NFATc) pathway (Arron et al., 2006). It has been hypothesized that *DYRK1A* and *RCAN1* overexpression in trisomy negatively regulates NFATc transcriptional activity via the direct phosphorylation of NFATc by DYRK1A and the inhibition of the NFAT dependent phosphatase, calcineurin, by RCAN1. These interactions are hypothesized to reduce the nuclear localization and, subsequently NFATc

transcriptional activity in specific cell types. NFATc has been shown to be involved in both osteoblast and osteoclast development (Winslow et al., 2006; Zhao et al., 2010), and its activity was significantly reduced in bone marrow mesenchymal cells isolated from the bones of *Dyrk1a* overexpressing transgenic mice (Lee et al., 2009). Furthermore, *Dyrk1a* overexpressing transgenic mice exhibit severe bone abnormalities similar to those observed in Ts65Dn mice (Blazek et al., 2011; Lee et al., 2009), suggesting *Dyrk1a* as a candidate gene for the development of DS associated bone abnormalities.

Based on the findings that several Ts65Dn phenotypes originate during embryonic development and the evidence suggesting *Dyrk1a* overexpression affects appendicular bone development, we hypothesized that the Ts65Dn postnatal phenotype originates during prenatal development in a *Dyrk1a* dependent manner. To test this hypothesis, we assessed embryos from Ts65Dn mice at embryonic day (E) 13.5, E14.5, and E17.5, and from Ts65Dn, *Dyrk1a*$^{+/-}$ mothers (containing only two functional copies of *Dyrk1a*) at E13.5 and E17.5. Our data suggest that the Ts65Dn postnatal appendicular bone phenotype begins as early as E17.5 with a reduction in percent bone volume; however, no abnormalities were observed in the establishment or development of the cartilage template during the embryonic processes of endochondral ossification. *Dyrk1a* copy number variation and transcript expressions were not significantly correlated with the prenatal Ts65Dn appendicular skeletal phenotype. These data suggest that trisomic *Dyrk1a* is not a significant contributor to the abnormal embryonic development of the Ts65Dn femur, and by extension, the appendicular skeleton.

2. Results

2.1 Trisomy affects bone mineralization at E17.5 in the Ts65Dn femur

To determine if the postnatal Ts65Dn appendicular skeletal phenotype originates during embryonic development with the involvement of *Dyrk1a*, bone analyses were conducted on femurs from E13.5, E14.5, and E17.5 embryos in several comparative sets of mice. Bone microarchitecture was evaluated in Ts65Dn (n=13) and euploid (n=10) embryos isolated from Ts65Dn mothers (Figure 1), like those used in the original postnatal skeletal study (Blazek et al., 2011). Additionally, to determine if *Dyrk1a* copy number influences prenatal femoral development, bone microarchitecture was assessed in offspring of Ts65Dn mice bred with *Dyrk1a*$^{+/-}$ mice (containing only one functional copy of the *Dyrk1a* gene) resulting in four possible genotypes: Ts65Dn (n=9), Ts65Dn, *Dyrk1a*$^{+/-}$ (Ts65Dn with two functional copies of *Dyrk1a*; n=12), euploid (n=8), and euploid, *Dyrk1a*$^{+/-}$ (one functional copy of *Dyrk1a*; n=9) embryos (Figure 1).

Micro-CT (μCT) analysis of E17.5 femurs revealed Ts65Dn embryos exhibited a significantly lower percent bone volume (BV/TV; bone volume/total femur tissue volume) in the developing femur when compared to euploid embryos (Figure 1C,D). Despite having only two functional copies of *Dyrk1a,* Ts65Dn, *Dyrk1a*$^{+/-}$ E17.5 femurs had a similar percent bone volume in the femoral primary ossification center when compared to Ts65Dn embryos and this value was significantly lower compared to euploid embryos (Figure 1D). Euploid, *Dyrk1a*$^{+/-}$ embryo femurs exhibited lower percent bone volume as compared to euploid femurs, but this value was not statistically significant (p=0.09; Figure 1D).

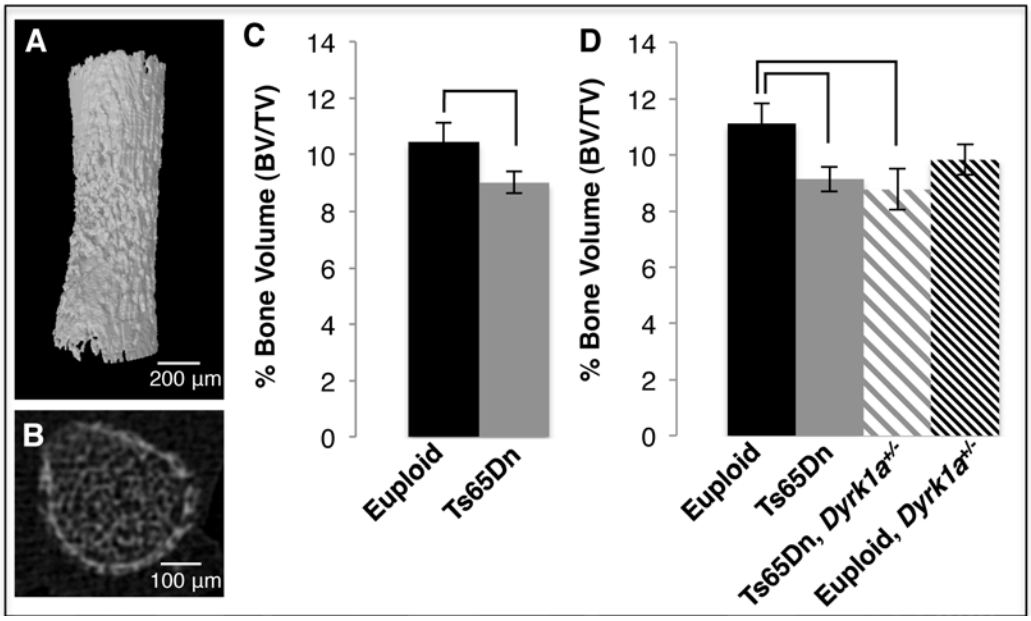

Figure 1: A 3D-reconstruction (A) and cross-section (B) taken from µCT analysis of the E17.5 femoral primary ossification center. 3D analysis of percent bone volume in the E17.5 primary ossification center revealed a significantly lower bone volume per tissue volume in Ts65Dn and Ts65Dn, *Dyrk1a*$^{+/-}$ embryos when compared to euploid (C,D). Mean ±SEM; bars between groups of mice denote significance with a p-value < 0.05.

2.2 Expression of Dyrk1a is independent of changes in Ts65Dn E17.5 femur bone mineralization

Dyrk1a and *Rcan1* are found in three copies in the Ts65Dn mouse model and are theoretically expected to be overexpressed approximately 1.5 fold. To determine if expression of *Dyrk1a* and *Rcan1* transcripts are altered by trisomy and contribute to the reduction in bone mineralization found at E17.5, RNA from the femoral primary ossification center of E17.5 euploid, Ts65Dn, Ts65Dn, *Dyrk1a*$^{+/-}$, and euploid, *Dyrk1a*$^{+/-}$ embryos were assessed. Quantitative PCR (qPCR) analysis of cDNA from the femoral primary ossification center of Ts65Dn and euploid E17.5 embryos revealed that *Dyrk1a* and *Rcan1* transcripts were elevated in Ts65Dn embryos (Figure 2), although *Rcan1* was not significantly different from euploid (p=0.095). Ts65Dn, *Dyrk1a*$^{+/-}$ embryonic femurs exhibited significantly lower *Dyrk1a* transcript levels when compared to Ts65Dn (p = 0.02) and these were similar to those observed in the euploid embryonic femur (~1.03 fold). *Rcan1* transcripts were increased in Ts65Dn, *Dyrk1a*$^{+/-}$ compared to Ts65Dn embryos but this increase was not significant (p=0.06). Euploid, *Dyrk1a*$^{+/-}$ embryos containing only one functional copy of *Dyrk1a* exhibited a significant decrease in *Dyrk1a* transcripts (0.54 fold, p=0.004) in the primary ossification center as compared to euploid

embryos (Figure 2). *Dyrk1a* RNA transcript levels in brain tissue of similarly aged offspring were comparable to those found in femur for all embryonic genotypes, and RNA transcript levels for Rcan1 were ~1.5 fold euploid in both Ts65Dn and Ts65Dn, *Dyrk1a*$^{+/-}$ and not significantly different from euploid levels in euploid, *Dyrk1a*$^{+/-}$ brain.

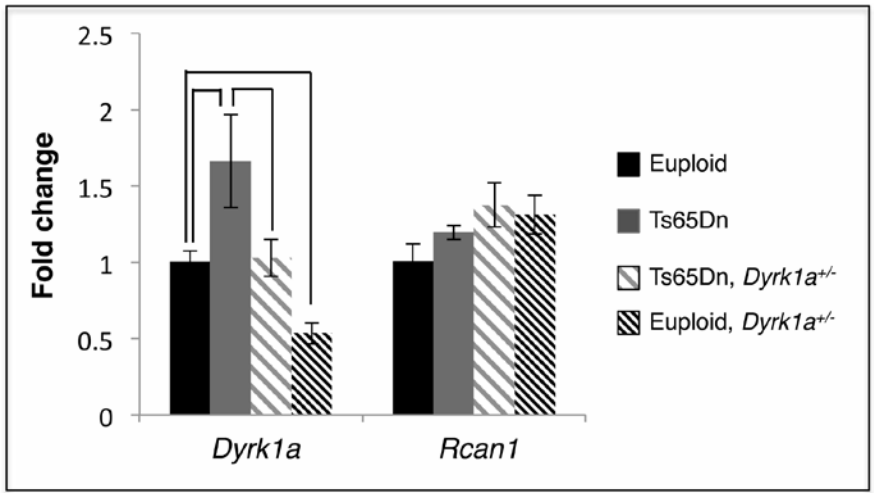

Figure 2: qPCR analysis of cDNA from the primary ossification center transcripts of E17.5 Ts65Dn (n=3), Ts65Dn, *Dyrk1a*$^{+/-}$ (n=3), euploid, *Dyrk1a*$^{+/-}$ (n=3) and euploid (n=3) embryos indicate that *Dyrk1a* transcripts were significantly overexpressed in Ts65Dn when compared to euploid embryos. Depicted *Dyrk1a* results are from target Mm01209880_m1 and qPCR from Mm00432929_1 gave similar results. *Rcan1* transcripts were increased in the primary ossification center of these embryos, however, these increases were not significant. Mean normalized to euploid levels ±SEM. Bars between groups of mice denote a p-value < 0.05.

2.3 Nfatc cellular localization is unaffected by trisomy in embryonic femoral cartilage anlagen

Based on the finding of a reduced percent bone volume in the primary ossification center of E17.5 Ts65Dn embryos and increased expression of both *Dyrk1a* and *Rcan1* transcripts, it was hypothesized that NFATc1 or NFATc2 activity would be reduced in the bone precursor of Ts65Dn embryos. To further assess if the *Dyrk1a*-*Rcan1*-NFAT pathway is involved in the abnormal prenatal development of the femur in Ts65Dn mice, immunofluorescent analysis was conducted to evaluate the cellular localization of NFATc1 and NFATc2 in the developing femur of Ts65Dn and euploid embryos. We assessed NFATc1/2 localization in the developing femur during the beginning stages of endochondral ossification at E13.5. Analysis of the cartilage anlagen in the femoral precursor of E13.5 Ts65Dn and euploid embryos revealed no significant differences in NFATc1 or NFATc2 nuclear localization (active form) (Figure 3).

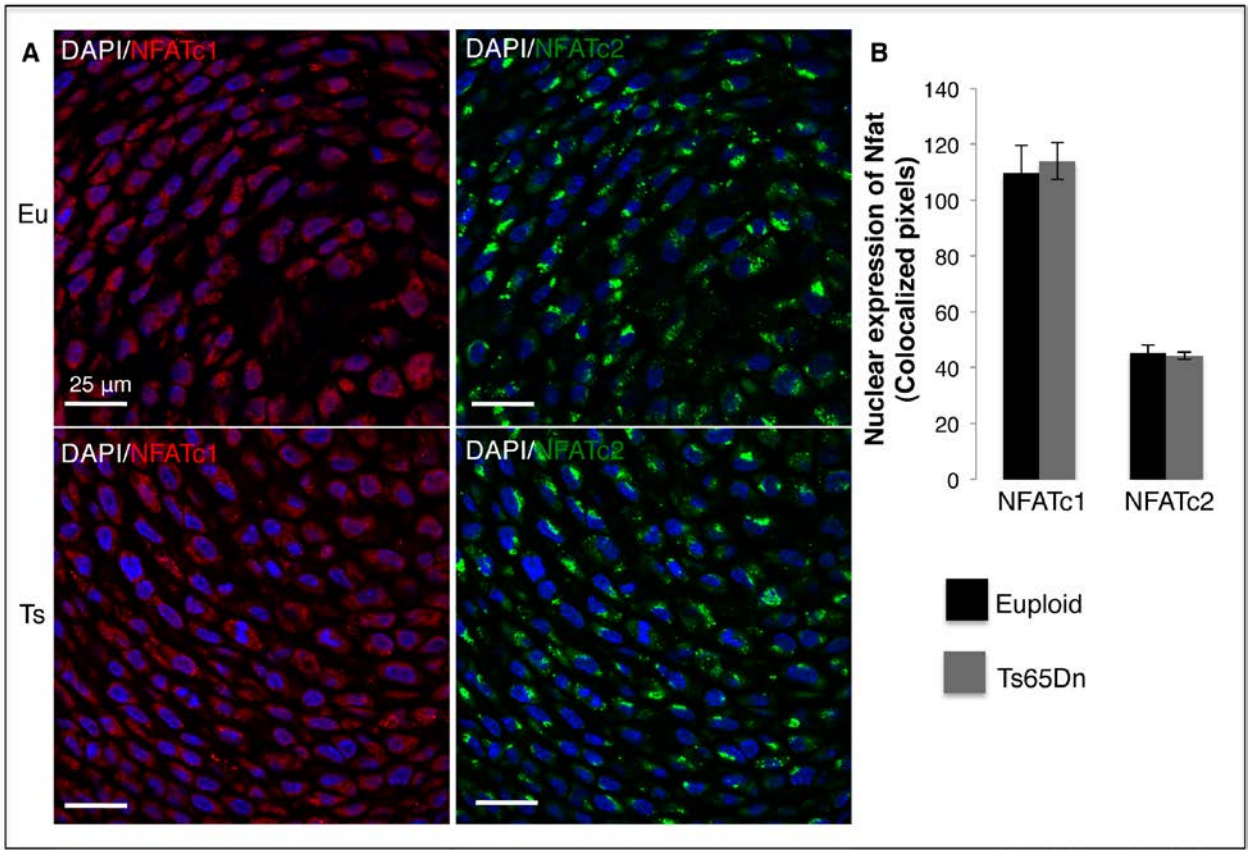

Figure 3: Immunofluorescent analysis of nuclear NFATc1 and NFATc2 in the E13.5 femoral cartilage anlagen was conducted using confocal imaging (A, images taken at 80x). (B) No significant differences were observed in the nuclear localization (active form) of NFATc1 or NFATc2 in the cartilage anlagen of the developing femur in Ts65Dn embryos (n=6) when compared to euploid embryos (n=6). Mean pixels colocalized with DAPI ±SEM.

2.4 The cartilage template is unaffected in the Ts65Dn embryonic femur

The formation of the femur occurs via a process of endochondral ossification, where a cartilage template precedes the formation of bone. The cartilage template is composed of zones of chondrocytes, or cartilage cells, which extend outward toward the growth plate. This process begins between E12.5 and E13.5 and proceeds through development until the bones have matured (Kauffman, 1992). Based on the abnormal phenotype observed in postnatal Ts65Dn mice and the reduction in percent bone volume observed at E17.5, we hypothesized that trisomy and/or *Dyrk1a* overexpression affects development of the cartilage template and the processes of endochondral ossification. Using histological staining, we assessed the lengths of the embryonic femur, primary ossification center, proliferative zone of chondrocytes (PZ; area where chondrocytes are proliferating thereby creating the growth plate), and zone of hypertrophic

chondrocytes (HZ; an area where chondrocytes are undergoing hypertrophy making way for osteoblasts to mineralize bone) to analyze the developing cartilage template and femur in Ts65Dn embryos (Figure 4). No significant differences were found in the length of the femur or the length (Figure 4C,F) or width (data not shown for E17.5) of the hypertrophic chondrocyte zone at either E14.5 or E17.5 in the Ts65Dn femur when compared to euploid mice. Furthermore, no differences were observed in the length of the primary ossification center, or proliferative zone between Ts65Dn and euploid mice in either group at E17.5 (Table 1). Return of *Dyrk1a* copy number to normal levels in Ts65Dn, *Dyrk1a*$^{+/-}$ mice did not alter any of the embryonic femoral template parameters at E17.5 (Table 1). Euploid, *Dyrk1a*$^{+/-}$ embryos exhibited a significantly shorter HZ when compared to the other three genotypes and this difference still existed when HZ length was normalized with femur length and compared to euploid or Ts65Dn, *Dyrk1a*$^{+/-}$ mice (Table 1).

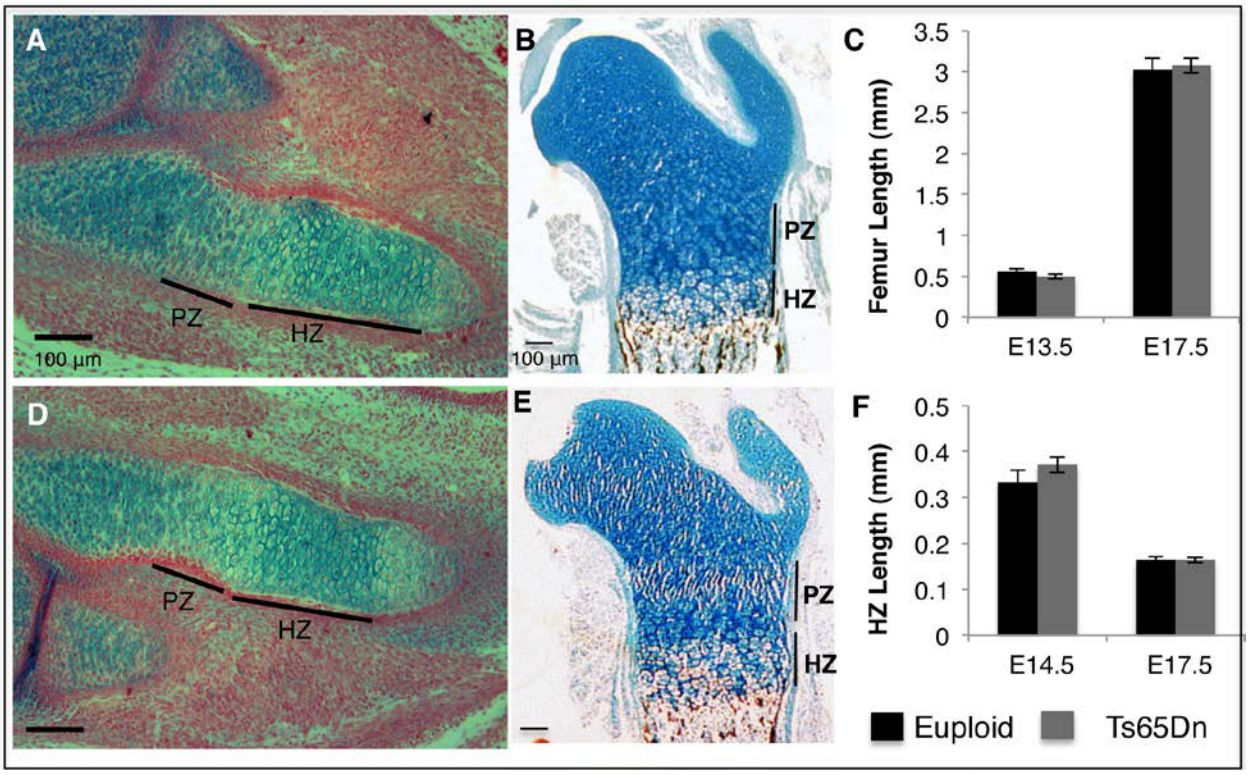

Figure 4: Histological analysis of the cartilage template in euploid (A,B) and Ts65Dn (D,E) limbs at E14.5 (A,D) and E17.5 (B,E). Mean femur length (±SEM) was measured in Ts65Dn (E13.5, n=17; E17.5, n = 13) and euploid (E13.5, n = 11; E17.5 n = 12) (C). The zones of developing chondrocytes include the hypertrophic zone (HZ) and proliferative zone (PZ) shown and the HZ was measured and compared in Ts65Dn (E14.5, n = 4; E17.5, n = 10) and

euploid (E14.5, n =4; E17.5, n = 13) embryos. No significant difference was observed in the length of the HZ between the two genotypes at either time point (F).

Table 1: Analysis of the E17.5 femoral template in offspring from Ts65Dn, *Dyrk1a*$^{+/-}$ mice

	Euploid n=8	Ts65Dn n=9	Ts65Dn, *Dyrk1a*$^{+/-}$ n=12	Euploid, *Dyrk1a*$^{+/-}$ n=9
Femur Length (mm)	3.14 (0.08)	3.16 (0.1)	3.08 (0.07)	3.14 (0.08)
Primary OC (mm)	1.13 (0.07)	1.17 (0.06)	1.13 (0.04)	1.09 (0.06)
POC/Bone Length (%)	35.94 (1.89)	36.74 (0.63)	36.75 (1.01)	34.68 (1.37)
HZ Length(mm)	0.161 (0.005)	0.156 (0.004)	0.154 (0.002)	0.147 (0.002)^{A,B,C}
HZ/Bone Length (%)	5.16 (0.26)	4.97 (0.22)	5.06 (0.12)	4.72 (0.15)^{A,C}
PZ Length (mm)	0.274 (0.008)	0.265 (0.010)	0.273 (0.006)	0.271 (0.007)
PZ/Bone Length (%)	8.76 (0.37)	8.41 (0.33)	8.95 (0.19)	8.67 (0.32)

Data are reported as mean (±SEM); OC (ossification center), HZ (hypertrophic chondrocyte zone), PZ (Proliferative zone); ^{A} $p < 0.05$ when compared to euploid, ^{B} $p < 0.05$ when compared to Ts65Dn, ^{C} $p < 0.05$ when compared to Ts65Dn, *Dyrk1a*$^{+/-}$.

To further assess the development of the cartilage anlagen in Ts65Dn mice immunohistochemistry was performed on E14.5 embryos to identify the expression of the cartilage specific proteins collagen II (differentiated chondrocytes) and collagen X (hypertrophic chondrocytes). These proteins are temporally expressed in a sequential pattern during the progression of endochondral ossification. As suggested by the findings above, no discernible differences were found in the distribution of collagen II or X when comparing the forelimbs of Ts65Dn (n = 5) and euploid (n = 5) embryos. These proteins were localized to the extracellular matrix and found within the expected regions of the developing limb (Figure 5).

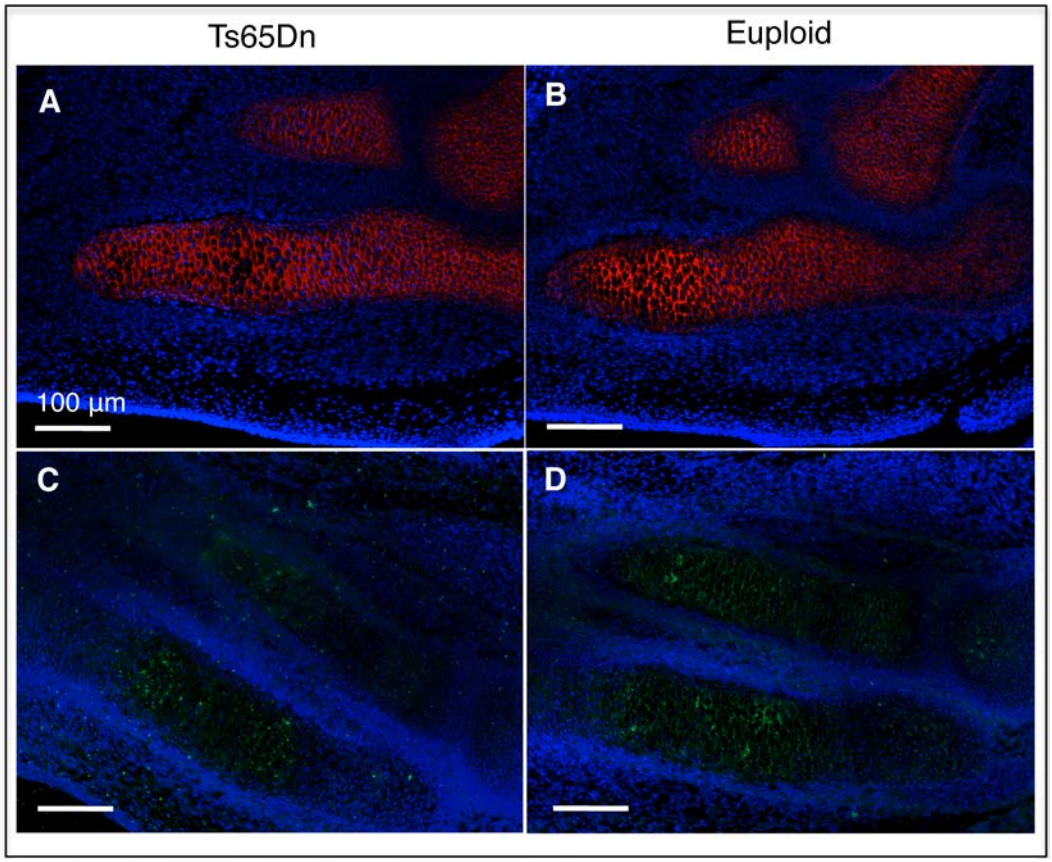

Figure 5: For both Ts65Dn (n=5; A,C) and euploid embryos (n=5, B.D), 8µm section were analyzed using fluorescent immunohistochemistry to visualize the pattern of expression of collagen II in red (A, B) and collagen X in green (C, D) within the developing forelimb. Tissue sections were counterstained with DAPI (blue).

3. Discussion

Ts65Dn mice exhibit an osteopenic postnatal appendicular skeletal phenotype (Blazek et al., 2011) similar to that documented in humans with DS (Baptista et al., 2005; de Moraes et al., 2008), and it has been hypothesized that these phenotypes originate during embryonic development of the skeleton. Additionally, due to its presence in three copies, subsequent overexpression, and involvement in several critical developmental signaling pathways, *Dyrk1a* has been hypothesized to be a contributing gene in a number of DS phenotypes including cognitive impairment (Haydar and Reeves, 2012), Alzheimer disease (Kimura et al., 2007; Wegiel et al., 2008), and abnormal skeletal development (Arron et al., 2006; Lee et al., 2009). In this work, we set out to determine if the abnormal Ts65Dn postnatal bone phenotype originates during embryonic development and the role, if any, that *Dyrk1a* copy number variation plays in

the development of this phenotype. We hypothesized that Ts65Dn mice would exhibit significant alterations in prenatal bone development compared to euploid embryos and that overexpression of *Dyrk1a* transcripts due to trisomy of the gene would play a major role in the development of the abnormal prenatal bone phenotype.

μCT analysis of E17.5 femurs revealed a significantly lower percent bone volume in the developing Ts65Dn embryo when compared to euploid. Return of *Dyrk1a* copy number to euploid levels in Ts65Dn, *Dyrk1a*$^{+/-}$ mice did not affect percent bone volume in the embryonic femur. The lower percent bone volume observed in the E17.5 primary ossification center in Ts65Dn and Ts65Dn, *Dyrk1a*$^{+/-}$ embryos suggests that alterations in bone cell number or activity begin during embryonic development and likely contribute to the postnatal Ts65Dn appendicular skeletal phenotype. It is possible that osteoblast activity is decreased in the E17.5 primary ossification center similar to what was observed in postnatal Ts65Dn mice, leading to a slower rate of mineralization and the phenotype observed. Alternatively, there may be deficiencies in cellular recruitment and/or differentiation of osteoblasts in the E17.5 primary ossification center resulting in the lower percent bone volume at this developmental stage. To determine the role of osteoblast number and/or activity in the development of the E17.5 femoral phenotype, a dynamic bone analysis utilizing fluorescent dyes that incorporate into newly formed bone material in Ts65Dn embryos could be performed. Dyes injected into the mother 2 or 3 days apart when bone just begins to form (e.g. E13.5 and E15.5) would allow for the analysis of osteoblast number and activity in the E17.5 embryos.

qPCR analysis revealed that despite measurable reduction in percent bone volume, *Dyrk1a* transcripts were expressed at the expected euploid levels in the embryonic primary ossification center in Ts65Dn, *Dyrk1a*$^{+/-}$ femurs. Euploid, *Dyrk1a*$^{+/-}$ mice containing only one functional copy of the gene exhibited the predicted reduction in *Dyrk1a* transcript levels (0.54 fold) as compared to euploid embryos and percent bone volume was not significantly affected. A reduction in *Dyrk1a* transcripts did correlate with changes in the HZ in the euploid, *Dyrk1a*$^{+/-}$ femoral template. A trend toward higher *Rcan1* transcript expression in the Ts65Dn and Ts65Dn, *Dyrk1a*$^{+/-}$ and euploid, *Dyrk1a*$^{+/-}$ embryonic femurs may be correlated to the significantly lower percent bone volume in femurs from E17.5 embryos, but will require further evaluation with additional embryos. These results highlight a potential critical role for gene dosage compensation in a temporal and spatial manner in the developing Ts65Dn embryonic femur and

suggest that other gene(s) found in three and two copies are likely involved the establishment of the altered appendicular bone phenotype at this time point. The lower percent bone volume observed in Ts65Dn and Ts65Dn, *Dyrk1a*$^{+/-}$ embryos suggests that changes in *Dyrk1a* transcript levels do not directly affect the development of the abnormal embryonic appendicular bone phenotype observed in Ts65Dn mice at E17.5. Though RNA transcript levels were not quantified as in the present experiment, a similar gene dosage reduction experiment found that three copies of *Ets2* was not sufficient to fully cause hypothesized DS-related craniofacial and thymus phenotypes in Ts65Dn mice (Hill et al., 2009).

The abnormal bone phenotype identified in adolescent Ts65Dn mice suggested that trisomy may alter bone during embryonic development and the critical processes of endochondral ossification. The establishment of the cartilage template is critical during this phase of development and previous research suggests that key cartilage related genes, including *Sox9* and the hedgehog family, are affected by the presence of trisomy (Billingsley et al., 2013; Roper et al., 2009). Assessment of the embryonic endochondral cartilage template revealed no differences in the length or size of the zones of chondrocyte development between Ts65Dn and euploid embryos at E14.5 or E17.5, nor in the temporal expression of the cartilage markers collagen II and X at E14.5. Unlike in humans with DS, where shortened long bones have been identified during fetal development, the overall femoral length (E13.5 and E17.5) and primary ossification center (E17.5) were not affected by trisomy in Ts65Dn mice. These findings suggest that other trisomic genes found in Ts21, but not triplicated in Ts65Dn mice, may play a role in the development of the abnormal appendicular bone phenotype associated with DS during prenatal bone development. Though percent bone volume is affected by trisomy, our results suggest that the patterning of the cartilage template and the lengthening of the embryonic bone during the initial stages of endochondral ossification are not affected by trisomy in the Ts65Dn embryonic femur.

Here we are the first to report that percent bone volume is altered at E17.5 in the developing Ts65Dn femur and this is likely the onset to the abnormal bone phenotype observed in the postnatal Ts65Dn skeleton. Postnatal Ts65Dn mice exhibit an osteopenic appendicular skeletal phenotype with lower bone mineral density, deficiencies in mineralization, and altered structural characteristics when compared to euploid mice (Blazek et al., 2011). Cellular analysis of the Ts65Dn femur identified a decreased number of osteoblasts and osteoclasts in the femur at

12 weeks of age (Fowler et al., 2012), and our further research has shown that osteoclast number is affected in adolescent Ts65Dn bone (unpublished data). These results suggest that the cellular activity of bone is affected during the onset of primary spongiosa development and the establishment of the marrow cavity. As the bone matures and more osteoblasts and osteoclasts are recruited to the developing ossification front, these abnormalities may become more severe leading to the phenotype observed at 6 weeks of age in the Ts65Dn femur.

Contrary to what was hypothesized, the *Dyrk1a-Rcan1*-NFAT pathway does not appear to directly affect the embryonic development of the appendicular skeleton in Ts65Dn mice, despite overexpression of *Dyrk1a* transcripts in the embryonic Ts65Dn femur. We did not find evidence to support the hypothesis that triplication of *Dyrk1a* and *Rcan1* inhibits NFAT functionality by reducing nuclear localization. No differences in NFATc1 or 2 protein in the nuclei were detected in trisomic embryos at E13.5. However, we cannot rule out that NFAT function may affect trisomic bone development at later time points, either pre- or postnatally or that other NFATc family members may be involved in transcriptional regulation in the cartilage primordia at this developmental stage. Furthermore, the lack of differences in femur length and length of the primary ossification center in Ts65Dn and euploid embryos suggest that the critical developmental changes leading to the abnormal Ts65Dn appendicular skeleton occur during the processes of postnatal bone development. Concurrent research is being conducted to further assess the role of *Dyrk1a* copy number on the postnatal development of the Ts65Dn postnatal phenotype and to identify the mechanism by which this phenotype occurs.

4. Materials and Methods:

4.1 Animals

Female B6EiC3Sn a/A-Ts(17^{16})65Dn (Ts65Dn) and male C57BL6/J and C3H/HeJ stocks used in this study were originally obtained from The Jackson Laboratory (Bar Harbor, ME). Ts65Dn females used as mothers in this study were generated by matings with $B6C3F_1$ males at Indiana University-Purdue University Indianapolis (IUPUI) or Franklin and Marshall College and were identified by FISH (Moore et al., 1999) or PCR genotyping (Reinholdt et al., 2011). B6129 *Dyrk1a*$^{+/-}$ male mice (Fotaki et al., 2002) were backcrossed to B6C3F1 mice for ≥7 generations to parallel the genetic background of Ts65Dn mice. To obtain embryos for this study

Ts65Dn mothers were bred to male B6C3F1 or Wnt1-cre mice on a B6 background (for E13.5-E17.5 studies) or male *Dyrk1a*$^{+/-}$ mice (E17.5) and mothers were checked for vaginal plugs the morning after mating with E0.5 defined as 12:00 pm on the day the female was plugged. Embryos were genotyped for trisomy and mutant *Dyrk1a* as previously described (Fotaki et al., 2002). All animal use and protocols were approved by the IACUC committees at IUPUI and Franklin and Marshall College.

4.2 Processing of Embryos

Ts65Dn mothers carrying embryos were sacrificed at E13.5, 14.5, or 17.5 days post-conception and embryos were subjected to fixative or hypothermia. For immunofluorescence, E13.5 embryos were decapitated and the head and torso were embedded separately. Briefly, embryos were fixed in 4% paraformaldehyde, 5% sucrose in 0.1M phosphate buffer ph 7.4 for 4 hours and infiltrated overnight with 20% sucrose in phosphate buffer for cryo-embedding. For paraffin embedding of E14.5, embryos were decalcified with EDTA for three days, serially dehydrated, and embedded in paraffin. Cryo-embedded torsos were stored at -80°C and sectioned using a cryostat at a thickness of 10 μm. Paraffin embedded embryos were sectioned on a microtome at 8 μm and stored at room temp. The left and right femurs were dissected from E17.5 embryos, washed with PBS, and fixed overnight in 4% paraformaldehyde. Femurs were washed with PBS, dehydrated using sequential alcohol washes, cleared with xylenes, and embedded in paraffin and stored at 4°C. Embryos were sectioned on a microtome at a thickness of 10 μm.

4.3 Immunofluorescence

Torso sections of E13.5 and E14.5 Ts65Dn and euploid embryos were examined for the cellular localization of Nfatc1 and Nfatc2, and Collagen II and X, respectively, in the cartilage primordia of the limb. For analysis of E13.5 embryos, sections were permeabilized in 1X PBS with 0.5% triton X-100, washed in 1X PBS with 5% SDS for antigen retrieval, blocked with 10% donkey serum in PBS with 0.2% triton X-100 for 1 hour, and treated with Rabbit polyclonal Nfatc1 (sc-13033, dilution 1:20, SCBT) and goat polyclonal Nfatc2 (CSC-1151, dilution 1:20, SCBT) diluted in blocking buffer overnight in a humidified chamber at 4°C. Sections were washed and incubated with secondary antibody (Alexaflour 594 donkey anti rabbit IgG

(Invitrogen A21207), 1:750 and Alexafluor 488 donkey anti goat IgG (Invitrogen A-11055), 1:750) for 1 hour at room temperature and treated with Prolong gold DAPI antifade (Invitrogen, P36935), coverslipped, and sealed with nail polish. Slides were imaged using an Olympus FV-111-MPE confocal multiphoton microscope (Olympus, Center Valley, PA). Colocalization of Nfatc1/2 and DAPI in the nuclei was analyzed using Image J software (National Institute of Health, Bethesda, MD) as previously described (Dunn et al., 2011). For E14.5 embryos, sections were digested with hyaluronidase, blocked, incubated overnight with primary antibody (rabbit polyclonal anti-collagen X (Abcam); mouse monoclonal collagen II (DSHB)) diluted 1/100 in blocking buffer, washed, and incubated with the secondary antibodies listed previously. Slides were viewed with a Leica DMRB and imaged using ProgRes CapturePro software (Jenoptik AG).

4.4 MicroCT imaging

Prior to embedding, femurs from Ts65Dn, Ts65Dn *Dyrk1a* +/-, euploid, and euploid *Dyrk1a* +/- E17.5 embryos were imaged using the Skyscan 1172 microCT and analyzed using the parameters and methods previously described (Blazek et al., 2011). The analysis of the reconstructed primary ossification center was slightly altered from the listed protocol as the region of interest included the entire ossification boundary of the embryonic femur. A 3D analysis was conducted to obtain the percent bone volume (a relative measure of total bone mineral present). Additionally, the length of the primary ossification center was measured and compared among groups of mice.

4.5 Histology

To determine if trisomy results in changes in the cartilage template of the E13.5, E14.5 and E17.5 femur, femur sections were subjected to Von Kossa (bone mineral) and alcian blue (chondrocytes) staining. For whole mount staining of E13.5 embryos were fixed in ethanol, stained with alcian blue (0.15%; Sigma, St. Louis), cleared with KOH in glycerol, washed, and imaged to obtain femur lengths using a Motic BA400 microscope, Moticam 2300 camera, and Motic software. For stained sections, slides were deparaffinized in Citrisolv (Fisher), rehydrated with sequential ethanol washed, treated with 1% silver nitrate under UV-light, and washed with 5% sodium thiosulfate to remove any unreacted silver. Sections were then incubated with 1%

alcian blue solution in acetic acid (pH 2.5), washed with DI water and cover-slipped with aqueous mounting media. Stained sections were imaged using the Nikon Ds-Fi1 Digital Sight camera and the length of the bone, primary ossification center, and zones of cartilage were analyzed using Image J software.

4.6 Quantitative PCR

RNA was isolated from mineralized bone from E17.5 femurs and cDNA conversion was conducted on 500 ng RNA from each sample using previously described methods (Deitz and Roper, 2011). qPCR was performed using Dyrk1a (Targets, Mm01209880_m1 and Mm00432929_m1 cover *Dyrk1a* exons 4-5 and 5-6, respectively, (NCBI Reference sequence NM_001113389.1), which correspond to exons 6-7 and 7-8 in the Dyrk1a genomic sequence depicted in Fotaki et al. 2002); *Rcan1* (Target, Mm01213406_m1 amplifying the 5'UTR region of the AF263240.1, AK010696.1, mCT169224.0, mCT169225.0 transcripts); and *Actinb* (endogenous, Mm00607939_s1 (Life Technologies)) primers using the manufacturer's instructions (TaqMan Gene Expression Assay, Applied Biosystems, Foster City, CA). The crossing point (Cp) values (done in triplicate) from each target primer were analyzed and normalized to the reference probe using the Applied Biosystems 7300 Real Time PCR System and software (Pfaffl, 2001). Average values for each primer were compared between euploid and Ts65Dn, Ts65Dn *Dyrk1a +/-*, or euploid *Dyrk1a +/-* embryos to compute the fold change in expression.

4.7 Statistical Analysis

Data were analyzed using an independent samples student T-test or ANOVA to compare means across groups using SPSS.

5. Acknowledgements

We are grateful to the Developmental Studies Hybridoma Bank for the use of the monoclonal antibody developed by T.F. Linsenmayer, created by the NICHD of the NIH and maintained at The University of Iowa, Department of Biology, Iowa City, IA 52242. We thank Emily Potts for her help dissecting and sectioning animals and Sam Deitz and Jeff Solzak for

their expertise and help in quantitative PCR.

6. References

Arron, J.R., Winslow, M.M., Polleri, A., Chang, C.P., Wu, H., Gao, X., Neilson, J.R., Chen, L., Heit, J.J., Kim, S.K., Yamasaki, N., Miyakawa, T., Francke, U., Graef, I.A. and Crabtree, G.R., 2006. NFAT dysregulation by increased dosage of DSCR1 and DYRK1A on chromosome 21. Nature. 441, 595-600.

Baptista, F., Varela, A. and Sardinha, L.B., 2005. Bone mineral mass in males and females with and without Down syndrome. Osteoporos Int. 16, 380-8.

Becker, W. and Joost, H.G., 1999. Structural and functional characteristics of Dyrk, a novel subfamily of protein kinases with dual specificity. Prog Nucleic Acid Res Mol Biol. 62, 1-17.

Billingsley, C.N., Allen, J.R., Baumann, D.D., Deitz, S.L., Blazek, J.D., Newbauer, A., Darrah, A., Long, B.C., Young, B., Clement, M., Doerge, R.W. and Roper, R.J., 2013. Non-trisomic homeobox gene expression during craniofacial development in the Ts65Dn mouse model of Down syndrome. Am J Med Genet A. 161A, 1866-74.

Blazek, J.D., Billingsley, C., Newbauer, A, Roper, R.J., 2010. Embryonic and not maternal trisomy causes developmental attenuation in the Ts65Dn mouse model for Down syndrome. Developmental Dynamics.

Blazek, J.D., Gaddy, A., Meyer, R., Roper, R.J. and Li, J., 2011. Disruption of bone development and homeostasis by trisomy in Ts65Dn Down syndrome mice. Bone. 48, 275-80.

Center, J., Beange, H. and McElduff, A., 1998. People with mental retardation have an increased prevalence of osteoporosis: a population study. Am J Ment Retard. 103, 19-28.

Davisson, M.T., Schmidt, C., Reeves, R.H., Irving, N.G., Akeson, E.C., Harris, B.S. and Bronson, R.T., 1993. Segmental trisomy as a mouse model for Down syndrome. Prog Clin Biol Res. 384, 117-33.

de Moraes, M.E., Tanaka, J.L., de Moraes, L.C., Filho, E.M. and de Melo Castilho, J.C., 2008. Skeletal age of individuals with Down syndrome. Spec Care Dentist. 28, 101-6.

Deitz, S.L. and Roper, R.J., 2011. Trisomic and allelic differences influence phenotypic variability during development of Down syndrome mice. Genetics. 189, 1487-95.

Deutsch, S., Lyle, R., Dermitzakis, E.T., Attar, H., Subrahmanyan, L., Gehrig, C., Parand, L., Gagnebin, M., Rougemont, J., Jongeneel, C.V. and Antonarakis, S.E., 2005. Gene expression variation and expression quantitative trait mapping of human chromosome 21 genes. Hum Mol Genet. 14, 3741-9.

Dunn, K.W., Kamocka, M.M. and McDonald, J.H., 2011. A practical guide to evaluating colocalization in biological microscopy. Am J Physiol Cell Physiol. 300, C723-42.

Epstein, C.J., 2001. Down Syndrome (Trisomy 21), in: C.R. Scriver, A.B., W. S. Sly, and D. Valle (Ed.), The Metabolic and Molecular Basis of Inherited Disease. McGraw-Hill, New York, pp. 1223-1256.

Fotaki, V., Dierssen, M., Alcantara, S., Martinez, S., Marti, E., Casas, C., Visa, J., Soriano, E., Estivill, X. and Arbones, M.L., 2002. Dyrk1A haploinsufficiency affects viability and causes developmental delay and abnormal brain morphology in mice. Mol Cell Biol. 22, 6636-47.

Fotaki, V., Martinez De Lagran, M., Estivill, X., Arbones, M. and Dierssen, M., 2004. Haploinsufficiency of Dyrk1A in mice leads to specific alterations in the development and regulation of motor activity. Behav Neurosci. 118, 815-21.

Fowler, T.W., McKelvey, K.D., Akel, N.S., Vander Schilden, J., Bacon, A.W., Bracey, J.W., Sowder, T., Skinner, R.A., Swain, F.L., Hogue, W.R., Leblanc, D.B., Gaddy, D., Wenger, G.R. and Suva, L.J., 2012. Low bone turnover and low BMD in Down syndrome: effect of intermittent PTH treatment. PLoS One. 7, e42967.

Gray, D.L., Dicke, J.M., Dickerson, R., McCourt, C. and Odibo, A.O., 2009. Reevaluating humeral length for the detection of fetal trisomy 21. J Ultrasound Med. 28, 1325-30.

Guijarro, M., Valero, C., Paule, B., Gonzalez-Macias, J. and Riancho, J.A., 2008. Bone mass in young adults with Down syndrome. J Intellect Disabil Res. 52, 182-9.

Haydar, T.F. and Reeves, R.H., 2012. Trisomy 21 and early brain development. Trends Neurosci. 35, 81-91.

Hill, C.A., Sussan, T.E., Reeves, R.H. and Richtsmeier, J.T., 2009. Complex contributions of Ets2 to craniofacial and thymus phenotypes of trisomic "Down syndrome" mice. Am J Med Genet A. 149A, 2158-65.

Kauffman, M.H., 1992. The Atlas of Mouse Development, 6 ed. Elsevier Academic Press, San Diego, CA.

Keeling, J.W., Hansen, B.F. and Kjaer, I., 1997. Pattern of malformations in the axial skeleton in human trisomy 21 fetuses. Am J Med Genet. 68, 466-71.

Kimura, R., Kamino, K., Yamamoto, M., Nuripa, A., Kida, T., Kazui, H., Hashimoto, R., Tanaka, T., Kudo, T., Yamagata, H., Tabara, Y., Miki, T., Akatsu, H., Kosaka, K., Funakoshi, E., Nishitomi, K., Sakaguchi, G., Kato, A., Hattori, H., Uema, T. and Takeda, M., 2007. The DYRK1A gene, encoded in chromosome 21 Down syndrome critical region, bridges between beta-amyloid production and tau phosphorylation in Alzheimer disease. Hum Mol Genet. 16, 15-23.

Lee, Y., Ha, J., Kim, H.J., Kim, Y.S., Chang, E.J., Song, W.J. and Kim, H.H., 2009. Negative feedback Inhibition of NFATc1 by DYRK1A regulates bone homeostasis. J Biol Chem. 284, 33343-51.

Longo, D., DeFigueiredo, D., Cicero, S., Sacchini, C. and Nicolaides, K.H., 2004. Femur and humerus length in trisomy 21 fetuses at 11-14 weeks of gestation. Ultrasound Obstet Gynecol. 23, 143-7.

Moore, C.S., 2006. Postnatal lethality and cardiac anomalies in the Ts65Dn Down syndrome mouse model. Mamm Genome. 17, 1005-12.

Moore, C.S., Lee, J.S., Birren, B., Stetten, G., Baxter, L.L. and Reeves, R.H., 1999. Integration of cytogenetic with recombinational and physical maps of mouse chromosome 16. Genomics. 59, 1-5.

Moore, C.S. and Roper, R.J., 2007. The power of comparative and developmental studies for mouse models of Down syndrome. Mamm Genome. 18, 431-43.

Parker, S.E., Mai, C.T., Canfield, M.A., Rickard, R., Wang, Y., Meyer, R.E., Anderson, P., Mason, C.A., Collins, J.S., Kirby, R.S. and Correa, A., 2010. Updated National Birth Prevalence estimates for selected birth defects in the United States, 2004-2006. Birth Defects Res A Clin Mol Teratol. 88, 1008-16.

Pfaffl, M.W., 2001. A new mathematical model for relative quantification in real-time RT-PCR. Nucleic Acids Res. 29, e45.

Reeves, R.H., Irving, N.G., Moran, T.H., Wohn, A., Kitt, C., Sisodia, S.S., Schmidt, C., Bronson, R.T. and Davisson, M.T., 1995. A mouse model for Down syndrome exhibits learning and behaviour deficits. Nat Genet. 11, 177-84.

Reinholdt, L.G., Ding, Y., Gilbert, G.J., Czechanski, A., Solzak, J.P., Roper, R.J., Johnson, M.T., Donahue, L.R., Lutz, C. and Davisson, M.T., 2011. Molecular characterization of the translocation breakpoints in the Down syndrome mouse model Ts65Dn. Mamm Genome. 22, 685-91.

Richtsmeier, J.T., Baxter, L.L. and Reeves, R.H., 2000. Parallels of craniofacial maldevelopment in Down syndrome and Ts65Dn mice. Dev Dyn. 217, 137-45.

Roper, R.J., St John, H.K., Philip, J., Lawler, A. and Reeves, R.H., 2006. Perinatal loss of Ts65Dn Down syndrome mice. Genetics. 172, 437-43.

Roper, R.J., VanHorn, J.F., Cain, C.C. and Reeves, R.H., 2009. A neural crest deficit in Down syndrome mice is associated with deficient mitotic response to Sonic hedgehog. Mech Dev. 126, 212-9.

Schrager, S., 2004. Osteoporosis in women with disabilities. J Womens Health (Larchmt). 13, 431-7.

Sturgeon, X. and Gardiner, K.J., 2011. Transcript catalogs of human chromosome 21 and orthologous chimpanzee and mouse regions. Mamm Genome. 22, 261-71.

van Allen, M.I., Fung, J. and Jurenka, S.B., 1999. Health care concerns and guidelines for adults with Down syndrome. Am J Med Genet. 89, 100-10.

Wegiel, J., Dowjat, K., Kaczmarski, W., Kuchna, I., Nowicki, K., Frackowiak, J., Mazur Kolecka, B., Wegiel, J., Silverman, W.P., Reisberg, B., Deleon, M., Wisniewski, T., Gong, C.X., Liu, F., Adayev, T., Chen-Hwang, M.C. and Hwang, Y.W., 2008. The role of overexpressed DYRK1A protein in the early onset of neurofibrillary degeneration in Down syndrome. Acta Neuropathol. 116, 391-407.

Weisz, B., David, A.L., Chitty, L., Peebles, D., Pandya, P., Patel, P. and Rodeck, C.H., 2008. Association of isolated short femur in the mid-trimester fetus with perinatal outcome. Ultrasound Obstet Gynecol. 31, 512-6.

Winslow, M.M., Pan, M., Starbuck, M., Gallo, E.M., Deng, L., Karsenty, G. and Crabtree, G.R., 2006. Calcineurin/NFAT signaling in osteoblasts regulates bone mass. Dev Cell. 10, 771-82.

Zhao, Q., Wang, X., Liu, Y., He, A. and Jia, R., 2010. NFATc1: functions in osteoclasts. Int J Biochem Cell Biol. 42, 576-9.